CrystEngComm

Accepted Manuscript

ROYAL SOCIETY OF CHEMISTRY

www.rsc.org/crystengcomm

ARTICLE TYPE www. rsc.org/xxxxxx | XXXXXXXX

Synthesis, Characterization, Crystal Structures and Thermal and Photoluminescence Studies of Dimethylpyrazine-Carboxylate Mixed Ligand Silver(I) Coordination Polymers with Various Multinuclear Silver Units†

Zhan-Hui Wang, Dan-feng Wang, Ting Zhang, Rong-bin Huang,* Lan-sun Zheng

Received Xth XXXXXXXXXX 20XX, Accepted Xth XXXXXXXXX 20XX
First published on the web Xth XXXXXXXXXX 200X
DOI: 10.1039/b000000x

Seven new silver(I) coordination compounds based on dimethylpyrazine (dmpyz), $[Ag_4(2,5-dmpyz)(ndc)_2]_n$, $[Ag_2(2,5-dmpyz)(pma)_{0.5}]_n$, $[Ag_4(2,3-dmpyz)_2(mpa)_2]_n$, $[Ag_2(2,3-dmpyz)(npa)]_n$, $[Ag(2,3-dmpyz)_{0.5}(opa)_{0.5}]_n$, $[Ag_6(2,3-dmpyz)_3(mpa)_3]_n$ and $[Ag_6(2,3-dmpyz)_2(tma)_2\cdot 5H_2O]_n$, have been synthesized and have been characterized by elemental analyses, IR spectra and single-crystal X-ray diffraction. In compound **1**, two types of Ag_4 units are linked by the organic ligands to three-dimensional supramolecular framework. Compound **2** also shows a 3D network based on a $[Ag_4O_2]$ six-membered rings. Compounds **3** and **6** are both 2D 4^4-sql nets, in which the Ag_4 units and Ag_6 units are observed, respectively. In compound **4**, the npa ligand adopts a $\mu_5-\eta^1:\eta^1:\eta^1:\eta^2$ mode to link zigzag Ag_4 SBUs, giving a 2D network. Compound **5** shows a 1D infinite silver chain clamped by the opa ligands. In **7**, six coordinated Ag(I) ions propagate to an infinite 1D silver strap and the 2,3-dmpyz and tma ligands link the silver strap into 3D framework. The high structural diversity of the compounds and the Ag units are highly dependent on the solvent and the coordination mode of carboxylate. The thermal stabilities and photoluminescence behaviours of the compounds were also discussed.

1 Introduction

There is an immense current interest among the structural and bioinorganic chemists to explore the coordination chemistry of coinage metal ions exploiting the semiconductor, luminescence, medicinal and structural properties.[1–10] The closed shell d^{10} electronic configuration of Ag(I) results in argentophilic interaction which plays an important role in constructing fascinating structures.[11–15] Despite the repulsion expected between two closed-shell metal cations, there are a number of examples of Ag(I) coordination compounds (CCs) with short Ag-Ag interactions that have been structurally characterized, ranging from dimers to intricate high-nuclearity clusters. The silver aggregates occur widely in silver-ethynide supramolecular synthon,[16–18] which may be due to the diverse coordination modes of the alkynyl moiety and the tendency to form argentophilic interaction. However, the silver clusters are relatively lack in silver-organic coordination polymers except for the silver-ethynide coordination compounds.

There are large numbers of coordination polymers reported in recent years with interesting structures and excellent properties. However, it is not exact science to predict structures as very many factors can dramatically change the framework structure and physical properties. At this stage, confidence in accomplishing this goal is based upon the sophisticated selection and utilization of suitable organic ligands.

In the previous literatures, many Ag(I) coordination polymers which rest on pyrazine and its derivatives were obtained, however the complicated silver units in the coordination polymers were seldom observed .[19–26] Based on above considerations, our interest has been focused on dimethylpyrazine-carboxylate mixed ligand silver coordination polymers in which various silver units formed by $Ag\cdots Ag$ interaction exit. Herein we focus on the self-assembly of silver (I) and pyrazine derivatives (2,3-dimethylpyrazine (2,3-dmpyz) and 2,5-dimethylpyrazine (2,5-dmpyz))combining aromatic carboxylates as auxiliary ligands and obtained seven novel CCs, namely, $[Ag_4(2,5-dmpyz)(ndc)_2]_n$ (**1**), $[Ag_2(2,5-dmpyz)(pma)_{0.5}]_n$ (**2**), $[Ag_4(2,3-dmpyz)_2(mpa)_2]_n$ (**3**), $[Ag_2(2,3-dmpyz)(npa)]_n$ (**4**), $[Ag(2,3-dmpyz)_{0.5}(opa)_{0.5}]_n$

* State Key Laboratory of Physical Chemistry of Solid Surface and Department of Chemistry, College of Chemistry and Chemical Engineering, Xiamen University, Xiamen, China. E-mail: rbhuang@xmu.edu.cn; Fax: +86-592-2183047

† Electronic Supplementary Information (ESI) available: [Table S1, Table S2, PXRD patterns, IR, TGA and parameters and figures of the $\pi\cdots\pi$ interactions. CCDC 943509, 943511,943514, 943515,977577-977579.]. See DOI: 10.1039/b000000x/

(**5**), $[Ag_6(2,3-dmpyz)_3(mpa)_3]_n$(**6**) and $[Ag_6(2,3-dmpyz)_2(tma)_2\cdot 5H_2O]_n$(**7**) (2,3-dmpyz = 2,3-dimethylpyrazine, 2,5-dmpyz = 2,5-dimethylpyrazine, H_2ndc = 1,4-naphthalenedicarboxylic acid, H_4pma = pyromellitic acid, H_2mpa = m-phthalic acid, H_2npa = 3-nitrophthalic acid, H_2opa = o-phthalic acid, H_3tma = trimesic acid, DMF = N,N'-dimethylformamide). Different kinds of silver clusters formed by $Ag\cdots Ag$ interactions were observed in the seven coordination compounds.

2 Experimental

2.1 Materials and methods

All chemicals and solvents used in the syntheses were of analytical grade and used without further purification. IR spectra were measured on a Nicolet Avatar 330 FTIR Spectrometer at the range of 4000 - 500 cm^{-1}. Elemental analyses were carried out on a CE instruments EA 1110 elemental analyzer. Photoluminescence spectra were measured on a Hitachi F-7000 Fluorescence Spectrophotometer (slit width: 5 nm; sensitivity: high). TG curves were measured from 25 to 800 °C on a SDT Q600 instrument at a heating rate 10 °C min^{-1} under the N_2 atmosphere (100 mL min^{-1}). X-ray powder diffractions were measured on a Rigaku Ultima IV diffractometer with Cu-Kα radiation.

2.2 Syntheses

2.2.1 $[Ag_4(2,5-dmpyz)(ndc)_2]_n$ **(1).** Ag_2O (23.1 mg, 0.1 mmol), H_2ndc (21.6 mg, 0.1 mmol) and 2,5-dmpyz (10.2 mg, 0.1 mmol) were dissolved in ethanol-DMF mixed solvent (6 mL, v/v: 3/3) under stirring. Then aqueous NH_3 solution (25%, 1 mL) was dropped into the mixture to give a clear solution under ultrasonic treatment. The resultant solution was allowed to evaporate slowly in darkness at room temperature for several days to give colourless crystals of **1**. (Yield: 75%, based on silver). Anal. Calc. (found) for $Ag_4C_{30}H_{20}N_2O_8$: C, 37.23 (37.15); H, 2.08 (2.01); N, 2.89 (2.91)%. IR (KBr): $\nu(cm^{-1})$ = 3417 (s), 1560 (s), 1461 (w), 1410 (s), 1367 (s), 1260 (w), 1211 (w), 1158 (w), 1120 (w), 1031 (w), 970 (w), 865 (w), 820 (m), 797 (m), 666 (w).

2.2.2 $[Ag_2(2,5-dmpyz)(pma)_{0.5}]_n$ **(2).** The synthesis of **2** was similar to that of **1**, but with H_4pma (25.4 mg, 0.1 mmol) in place of H_2ndc and using methanol-ethanol (6 mL, v/v: 3/3) as solvent. The resultant solution was allowed to evaporate slowly in darkness at room temperature for several days to give the yellow crystals of **2**. (Yield: 65%, based on silver). Anal. Calc. (found) for $Ag_2C_{11}H_9N_2O_4$: C, 29.43 (29.34); H, 2.02(2.10); N, 6.24 (6.27)%. IR (KBr):ν (cm^{-1}) =3388 (m), 1569 (s), 1485 (m), 1452 (w), 1420 (w), 1377 (s), 1325 (m), 1292 (m), 1159 (m), 1136 (m), 1058 (m), 1032 (m), 925 (m), 860 (m), 800 (m), 758 (m), 660 (m).

2.2.3 $[Ag_4(2,3-dmpyz)_2(mpa)_2]_n$ **(3).** The synthesis of **3** was similar to that of **1**, but with H_2mpa (16.6 mg, 0.1 mmol) in place of H_2ndc and with 2,3-dmpyz in place of 2,5-dmpyz. The resultant solution was allowed to evaporate slowly in darkness at room temperature for several days to give the yellow crystals of **3**. (Yield: 78%, based on silver). Anal. Calc. (found) for $Ag_4C_{28}H_{24}N_4O_8$: C, 34.46 (34.55); H, 2.48(2.44); N, 5.74 (5.71)%. IR (KBr):ν (cm^{-1}) =3419 (w), 1592 (m), 1540 (s), 1363 (s), 1170 (m), 1078 (w), 997 (w), 971 (w), 935 (w), 844 (w), 815 (w), 740 (s), 709 (s), 657 (m).

2.2.4 $[Ag_2(2,3-dmpyz)(npa)]_n$ **(4).** The synthesis of **4** was similar to that of **3**, but with H_2npa (21.1 mg, 0.1 mmol) in place of H_2mpa and using DMF-H_2O (6 mL, v/v: 3/3) as solvent. The resultant solution was allowed to evaporate slowly in darkness at room temperature for several days to give the colorless crystals of **4**. (Yield: 62%, based on silver). Anal. Calc. (found) for $Ag_2C_{14}H_{11}N_3O_6$: C, 31.55 (31.51); H, 2.08(2.11); N, 7.88 (7.93)%. IR (KBr):ν (cm^{-1}) =3334 (m), 3151 (m), 1569 (s), 1533 (s), 1432 (m), 1384 (s), 1209 (w), 1089 (w), 1000 (w), 866 (w), 827 (m), 775 (w), 715 (w), 649 (w).

2.2.5 $[Ag(2,3-dmpyz)_{0.5}(opa)_{0.5}]_n$ **(5).** The synthesis of **5** was similar to that of **3**, but with H_2opa (16.6 mg, 0.1 mmol) in place of H_2mpa and using acetonitrile-methanol (6 mL, v/v: 3/3) as solvent. The resultant solution was allowed to evaporate slowly in darkness at room temperature for several days to give the colorless crystals of **5**. (Yield: 68%, based on silver). Anal. Calc. (found) for $AgC_7H_6NO_2$: C, 34.46 (34.44); H, 2.48(2.51); N, 5.74 (5.69)%. IR (KBr):ν (cm^{-1}) =3396 (m), 3079 (w), 1569 (s), 1403 (s), 1261 (w), 1170 (m), 1083 (m), 998 (w), 854 (w), 831 (w), 761 (m), 730 (m), 692 (m), 651 (m).

2.2.6 $[Ag_6(2,3-dmpyz)_3(mpa)_3]_n$ **(6).** The synthesis of **6** was similar to that of **3**, but using methanol-DMF (6 mL, v/v: 3/3) as solvent. The resultant solution was allowed to evaporate slowly in darkness at room temperature for several days to give the colorless crystals of **6**. (Yield: 74%, based on silver). Anal. Calc. (found) for $Ag_6C_{42}H_{36}N_6O_{12}$: C, 34.46 (34.51); H, 2.48(2.44); N, 5.74 (5.71)%. IR (KBr):ν (cm^{-1}) =3373 (m), 1600 (m), 1546 (s), 1365 (s), 1261 (w), 1174 (m), 1076 (w), 997 (w), 973 (w), 935 (w), 904 (w), 844 (w), 815 (m), 740 (s), 709 (s), 655 (m).

2.2.7 $[Ag_6(2,3-dmpyz)_2(tma)_2\cdot 5H_2O]_n$ **(7).** The synthesis of **7** was similar to that of **3**, but with H_3tma (21.0 mg, 0.1 mmol) in place of H_2mpa and using DMF-H_2O (6 mL, v/v: 3/3) as solvent. The resultant solution was allowed to evaporate slowly in darkness at room temperature for several days to give the colorless crystals of **7**. (Yield: 79%, based on

silver). Anal. Calc. (found) for $Ag_6C_{30}H_{32}N_4O_{17}$: C, 26.34 (26.38); H, 2.36 (2.44); N, 4.10 (4.14)%. IR (KBr):ν (cm^{-1}) =3276 (m), 1610 (s), 1564 (s), 1427 (s), 1351 (s), 1170 (w), 1103 (w), 1006 (w), 983 (w), 931 (w), 767 (w), 723 (m).

2.3 X-ray crystallography

Single crystals of the compounds **1-7** with appropriate dimensions were chosen under an optical microscope and quickly coated with high vacuum grease (Dow Corning Corporation) before being mounted on glass fibres for data collections. Data for **1-7** were collected on a Rigaku R-AXIS RAPID Image Plate single-crystal diffractometer with graphite-monochromated Mo Kα radiation source (λ= 0.71073 Å) operating at 50 kV and 90 mA in ω scan mode. A total of $44 \times 5.00^\circ$ oscillation images were collected, each being exposed for 20 s. The cell refinements and data reductions for **1-7** were accomplished with the PROCESS-AUTO processing program.[27] Absorption correction was applied by correction of symmetry-equivalent reflections using the ABSCOR program.[28]

Cell parameters were retrieved using SMART software and refined with SAINT on all observed reflections. Data reduction was performed with the SAINT software and corrected for Lorentz and polarization effects. Absorption corrections were applied with the program SADABS .[29] In all cases, the highest possible space group was chosen. All structures were solved by direct methods using SHELXS-97[30] and refined on F^2 by full-matrix least-squares procedures with SHELXL-97[31] in Olex2.[32] Atoms were located from iterative examination of difference F-maps following least squares refinements of the earlier models. Hydrogen atoms were placed in calculated positions and included as riding atoms with isotropic displacement parameters 1.2-1.5 times U_{eq} of the attached C or N atoms. The hydrogen atoms attached to oxygen were refined with O-H = 0.85 Å, and U_{iso} (H) = 1.2U_{eq} (O). All structures were examined using the Addsym subroutine of PLATON[33] to assure that no additional symmetry could be applied to the models. Pertinent crystallographic data collections and refinement parameters are collated in Table 1. The bond lengths and angles of Ag$\cdots$Ag interaction for **1-7** are collated in Table 2. The parameters of $\pi\cdots\pi$ interactions in **1, 2 and 4** are shown in Table S1, ESI.†Selected bond lengths and angles for **1-7** are collated in Table S2. ESI.†

3 Results and discussions

3.1 General characterization

Powder X-ray diffraction (PXRD) has been used to check the phase purity of the bulk samples in the solid state. For complexes **1-7**, the measured PXRD patterns closely match the simulated patterns generated from the results of single-crystal diffraction data (Fig. S1, ESI.†), indicative of pure products. The IR spectra (Fig. S2, ESI.†) of complexes **1-7** also show characteristic absorption bands mainly attributed to the asymmetric (ν_{as} : *ca.* 1600 cm^{-1}) and symmetric (ν_s : *ca.*1385 cm^{-1}) stretching vibrations of the carboxylic groups. No band in the region $1690-1730$ cm^{-1} indicates complete deprotonation of the carboxylic groups,[34] which is consistent with the result of the X-ray diffraction analysis.

3.2 Structure descriptions

3.2.1 $[Ag_4(2,5-dmpyz)(ndc)_2]_n$ **(1).** Single crystal X-ray diffraction analysis reveals that complex **1** crystallized in the triclinic space group *P*-1. The asymmetric unit of complex **1** contains four crystallographically independent Ag(I) ion, two ndc and one dmpyz ligands. A view of the local coordination geometries around Ag(I) ions is shown in Fig. 1a. The Ag1 and Ag4, both coordinated by two O atoms from two ndc ligands, respectively, are located in approximately linear environments with angles of 171.38(15)° and 173.59(16)°, which slightly deviate from the ideal 180° due to Ag$\cdots$Ag interaction. Ag2 is bound to three O atoms and one N atom resulting in a distorted tetrahedral geometry, the distortion of the tetrahedron can be indicated by the calculated value of the τ_4 parameter introduced by Houser[35] to describe the geometry of a four-coordinated metal system, which is 0.67 for Ag2 (for perfect tetrahedral geometry, τ_4=1). The coordination environment of Ag3 can be described as a Y-shaped geometry which is constructed by one N atom (N2) and two O atoms from two carboxyl groups with the largest angle of 151.15(16)°. The Ag-N and Ag-O bond lengths fall in the expected range. The ndc anion acts as a bridging ligand with two bridging modes of $\mu_4-\eta^1:\eta^1:\eta^1:\eta^1$ and $\mu_5-\eta^2:\eta^1:\eta^1:\eta^1$. Notably, the distance between the silver atoms varies from 2.8383(8) to 3.3696 Å, being shorter than twice the van der Waals radius of silver ions (3.44 Å)[36] and suggesting the presence of significant argentophilic interactions.

As a result, two types of Ag_4 baskets are formed by the silvers atoms (Fig. 1c). One type of the Ag_4 baskets are linked by the ndc ligands with a $\mu_4-\eta^1:\eta^1:\eta^1:\eta^1$ bridging mode to generate a infinite 1D chain, however, the other type of the Ag_4 baskets form a 2D net with the assistance of ndc which adopts a $\mu_5-\eta^2:\eta^1:\eta^1:\eta^1$ bridging mode (Fig. 1b). Then the dmpyz ligands connect the 1D chains with the 2D nets extending the 2D sheet into 3D supramolecular framework (Fig. 1d). Weak aromatic $\pi\cdots\pi$ stacking interactions exist between the adjacent phenyl rings and pyrazines (Fig. S5, ESI.†).

3.2.2 $[Ag_2(2,5-dmpyz)(pma)_{0.5}]_n$ **(2).** When H_2ndc is replaced by H_4pma, we obtain a 3D coordination polymer

which crystallizes in the triclinic space group *P*-1. Each asymmetric unit is comprised of two Ag(I) ions, one dmpyz ligand and a half of pma anion. As shown in Fig. 2a, both Ag1 and Ag2 display square-pyramidal coordination geometry, completed by one N atoms from dmpyz ligand and four O atoms belonging to three pma anions, respectively. Addison has defined a geometric parameter τ_5[37] ($\tau_5 = [(\theta - \varphi)/60]$, where θ and φ are the angles between the donor atoms forming the basal plane in square-pyramidal geometry) to five-coordinate metal system as an index of the degree of distortion. The τ_5 parameters for Ag1 and Ag2 are 0.55 and 0.36, respectively (for ideal square-pyramidal geometry, τ_5 = 0). And the pma anions clamp Ag(I) ions to give a $[Ag_4O_2]$ six-membered rings. The distance of the Ag$\cdots$Ag interaction in the intrasubunit is 3.1697(9) Å.

As shown in Fig. 2b, the $[Ag_4O_2]$ rings are linked by pma anions with a $\mu_{12} - (\eta^1, \eta^3) : (\eta^2, \eta^2) : (\eta^3, \eta^1) : (\eta^2, \eta^2)$ bridging mode to form a 2D net. Consequently, the dmpyz ligands link the adjacent 2D polymeric sheets into a 3D supramolecular structure (Fig. 2c). The columns of $\pi\cdots\pi$ stacking between the alternating pyrazines and phenyl rings are formed along a-axis, which make a significant contribution to consolidate the 3D structure (Fig. S6, ESI.†).

3.2.3 $[Ag_4(2,3-dmpyz)_2(mpa)_2]_n$ **(3).** Complex **3** crystallizes in the orthorhombic crystal system with space group of $Pca2_1$. There are four crystallographically independent Ag(I) ions, two 2,3-dmpyz and two mpa in the asymmetric unit of **3** (Fig. 3a). The Ag1, Ag2 and Ag4 ions are similarly located in T-shaped geometries, completed by two O atoms belonging to two different mpa ligands and one N atom from 2,3-dmpyz ligand, respectively. Ag3 locates in the four-coordinated geometry, in detail, the Ag3 is coordinated by one N atom from 2,3-dmpyz and three O atoms from three different mpa ligands. The distortion of the tetrahedron can be indicated by the calculated value of the τ_4 parameter introduced by Houser[35] to describe the geometry of a four-coordinate metal system. And the τ_4 parameter is 0.66 for Ag3. The Ag-O and Ag-N bond lengths fall in the ranges of 2.194(8) - 2.579(7) and 2.394(9) - 2.421(9) Å, respectively. Notably, the distance between the silver atoms varies from 2.9507(12) to 3.1532(12) Å, being shorter than twice the van der Waals radius of silver ions (3.44 Å)[36]. Then, the versatile Ag-Ag weak interactions assemble these adjacent Ag atoms into Ag_4 units.

As shown in Fig. 3b, Ag1 and Ag4 atoms are bridged by μ_2-2,3-dmpyz ligands and $\mu_4 - \eta^1 : \eta^1 : \eta^1 : \eta^1$-mpa ligands to form a 2D infinite undulated sheet. At the same time, Ag2 and Ag3 atoms are also linked by μ_2-2,3-dmpyz ligands and $\mu_4 - \eta^1 : \eta^1 : \eta^1 : \eta^1$-mpa ligands to a 2D sheet which is parallel with the above one (Fig. 3c). Then the Ag1-Ag2 and Ag1-Ag3 interactions link the two kinds of 2D sheets into double layer (Fig. 3d).

3.2.4 $[Ag_2(2,3-dmpyz)(npa)]_n$ **(4).** Complex **4** is a 2D coordination polymer and crystallizes in space group $P2_1/c$. In the structure of **4**, as shown in Fig. 4a, there are two crystallographically independent Ag(I) ions, one 2,3-dmpyz and one npa ligand. Ag1 and Ag2 adopt tetrahedral and T-shaped geometries, respectively. The distortion of the tetrahedral geometry can be indicated by the calculated value of the τ_4 parameter[35] to describe the geometry of a four-coordinate metal system. The τ_4 parameter is 0.65 for Ag1. The maximum bond angle and sum of bond angles around Ag2 are 154.64(14) and 359.8(14)°, respectively. The Ag-N and Ag-O bond lengths fall in the ranges of 2.262(4)-2.277(4) and 2.133(4)-2.603(4)Å, respectively.

It is noteworthy that two different Ag-Ag interactions in **4** fall into the range of 3.0051(7)-3.1628(10)Å, which are not exceptional and agree with the previously reported values.[38–40] The 2,3-dmpyz ligands coordinate the Ag_4 units into chains along the *a* axis (Fig. 4b). And also the npa ligand adopts a $\mu_5 - \eta^1 : \eta^1 : \eta^2$ mode to link zigzag Ag_4 SBUs, giving a 2D network. As a result, the Ag atoms are linked by the 2,3-dmpyz and npa ligands to the resultant 2D coordination compound. Weak aromatic $\pi\cdots\pi$ stacking interactions exist between the adjacent phenyl rings and pyrazines reinforcing the resulting network (Fig. S7, ESI.†).

3.2.5 $[Ag(2,3-dmpyz)_{0.5}(opa)_{0.5}]_n$ **(5).** Complex **5** exhibits a 2D net containing an infinite silver wire. It crystallizes in the monoclinic crystal system with space group of *C*2/c. As shown in Fig. 5a, in the asymmetric unit of **5**, there exist one Ag(I) ion, a half of 2,3-dmpyz and opa ligand. The Ag1 adopts a T-shaped coordination configuration with two O atoms of opa in the horizontal direction. The coordination environment is completed by one N atom of 2,3-dmpyz in the axial direction forming a T-shaped unit. The Ag-N and Ag-O bond lengths fall in the ranges of 2.416(2) and 2.1891(18) -2.218(2) Å, respectively.

It is noteworthy that two different Ag-Ag interactions in **5** fall into the range of 2.9366(9)-3.2448(9) Å, which are not exceptional and agree with the previously reported values.[41–43] If neglecting all the ligands, the Ag(I) ions aggregate along the a axis into a chain (Fig. 5b). Then the carboxyl groups of the $\mu_4 - \eta^1 : \eta^1 : \eta^1 : \eta^1$-opa ligands clamp the Ag ions to make the silver chain more stable. The silver wires are connected to the 2D network by the 2,3-dmpyz ligands.

3.2.6 $[Ag_6(2,3-dmpyz)_3(mpa)_3]_n$ **(6).** Single-crystal X-ray diffraction analysis reveals that complex **6** crystallizes in the monoclinic space group $P2_1/c$ and is a 2D wavy 4^4-sql net. The asymmetric unit of **6** was comprised of six silver ions, three 2,3-dmpyz ligands and three mpa ligands. As shown in Fig. 6a, Ag1, Ag2, Ag5 and Ag6 all lie in nearly T-shaped geometry completed by two O atoms from two different mpa and one N atom from 2,3-dmpyz ligand. Ag3 is four-

coordinated by one N atom from 2,3-dmpyz ligand and three O atoms from three different mpa ligands to furnish a distorted tetrahedron geometry. The maximum and minimum bond angles for Ag3 are 159.3(3) and 91.5(3)°, respectively. The distortion of the tetrahedron can be indicated by the calculated value of the τ_4 parameter introduced by Yang et al.[35] to describe the geometry of a four-coordinate metal system, which is 0.67 (for ideal tetrahedron τ_4 = 1). The Ag4 is also located in a tetrahedral geometry and coordinated by one N atom from 2,3-dmpyz ligand and three O atoms from three mpa ligands, which the value of τ_4 is 0.68. The Ag-N and Ag-O bond lengths fall in the range 2.399(10) to 2.444(11) and 2.190(8) to 2.694(8) Å, respectively, which are comparable to the related coordination compounds.[44,45] The argentophilic Ag-Ag distances vary from 2.9297(19) to 3.3885(14) Å. Such distances are clearly indicative of the presence of $d^{10}-d^{10}$ interactions. Furthermore, such Ag-Ag interactions form two types of Ag_6 fragments. In type 1 Ag_6 unit, the Ag5-Ag5^i interaction links the two Ag_3-triangles (Ag3-Ag4-Ag5). Type 2 Ag_6 unit shows a chair-form structure which contains two coplanar Ag_3-triangles (Fig. 6b).

As shown in Fig. 6c, three crystallographic independent mpa ligands adopt the $\mu_6-\eta^1:\eta^1:\eta^2:\eta^2$ and $\mu_4-\eta^1:\eta^1:\eta^1:\eta^1$ modes to link the Ag_6 SBUs to form the 4^4-sql net. And also the Ag_6 SBUs in the above 2D net are connected by the 2,3-dmpyz to form another 4^4-sql net (Fig. 6d), giving the resulting structure (Fig. 6e).

3.2.7 $[Ag_6(2,3-dmpyz)_2(tma)_2\cdot 5H_2O]_n$ **(7).** Compound **7** exhibits a 1D infinite silver strap in the 3D framework. It crystallizes in the monoclinic crystal system with space group of $P2_1/c$. There are six crystallographically independent Ag(I) ions, two tma, two 2,3-dmpyz ligands and five lattice water molecules in the asymmetric unit of **7** (Fig. 7a). The Ag1 is located in a nearly linear geometry at the largest angle of 162.41(12)° and coordinated by one N atom from 2,3-dmpyz and one O atom from tma ligand. The Ag2 ion adopts a nearly T-shaped geometry completed by three O atoms from three different tma ligands. Ag3, Ag4 and Ag5 display distorted tetrahedral coordination geometries which τ_4 parameters are 0.76 for Ag3, 0.59 for Ag4 and 0.71 for Ag5. The Ag3 and Ag5 are both surrounded by one N atom from 2,3-dmpyz and three O atoms from three distinct tma. The Ag4 is surrounded by four O atoms from three different tma and one water molecule. The coordination environment of Ag6 can be described as a Y-shaped geometry which is constructed by two O atoms from one tma and one N atom with the largest bond angle of 163.79(11)°. The Ag-N and Ag-O bond distances are within the expected ranges, which arrange from 2.125(3) to 2.375(3) and 2.102(3) to 2.693(3) Å. The argentophilic Ag-Ag distances vary from 2.8531(5) to 3.3519(10) Å. Interestingly, all neighboring six coordinated Ag(I) ions propagate to an infinite 1D silver strap in which the Ag_6 units are connected by Ag1-Ag6 interactions (Fig. 7b). The silver straps are connected by the 2,3-dmpyz ligands to form a 2D net (Fig. 7c).

As shown in Fig. 7d, two crystallographic independent tma ligands adopt the $\mu_7-(\eta^1,\eta^2):(\eta^1,\eta^2):(\eta^1,\eta^1)$ and $\mu_7-(\eta^2,\eta^0):(\eta^2,\eta^1):(\eta^1,\eta^1)$ modes to link the silver straps to form 3D framework.

3.3 Effect of different solvent system and carboxylates ligands on assembly

As is shown in the descriptions above, seven novel Ag(I) CPs with the dmpyz and different carboxylates were successfully synthesized and characterized. Based on the X-ray analysis results, **1** is 3D molecule in which the carboxylates show two coordination modes. The $\mu_4-\eta^1:\eta^1:\eta^1:\eta^1$ ndc ligands link the Ag ions to form a 1D chain while the $\mu_5-\eta^2:\eta^1:\eta^1:\eta^1$ ndc ligands coordinate the Ag ions to form a 2D network. Effect of the ndc ligands are distinct due to their difference of the coordination modes. For **2**, the pma has four carboxyl groups evenly distributed on the benzene ring, so the silver ions can be linked to a 2D structure by them. In the presence of the same carboxylate ligand, but different solvent systems, compounds **3** and **6** are both 2D structures but the silver units in the compounds and the inter structures are very different. For **3**, the Ag-Ag interactions form one kind of Ag_4 unit. But in **6**, two types of Ag_6 units are formed by the argentophilic interaction. Compound **3** shows a double layer formed by two layers which has the same structure but different directions. Compound **6** exhibits multi-layer sandwich structure in which the two outer layers and the middle one are in the same structure but different directions. For **4** and **5**, both of the npa and opa have two carboxyl groups, but npa has a nitro group. The npa in **4** link the Ag_4 units to form a 2D network but the opa in **5** clamps the silver ions to form a infinite silver chain. In **7**, the tma shows two different coordination modes. The tma ligands coordinate the silver chains to 3D framework and also make the Ag-Ag interactions more stable.

3.4 The various silver units in the coordination polymers

Varying coordination number and flexible coordination geometries around Ag(I) including linear, trigonal, pyramidal, square planar, tetrahedral, and octahedral have made it a distinct metal node to synthesize macrocycles, polymetallic clusters and higher periodic coordination polymers.[46–51] The coordination number of the silver ions in **2** are both 5 for Ag1 and Ag2, so it is very hard to form complicated silver units due to space steric hindrance. Different kinds of Ag_4 units are observed in **1, 3** and **4**. The average coordination numbers for silver ions in these three polymers are almost equal, between 2 and 3. In complex **5**, the coordination number and geometry

for the silver ions are all same because there are only one silver ion in the asymmetric unit. Due to the simple geometry of Ag1, the 1D infinite silver chain was formed. The average coordination numbers and geometries of the silver ions in **6** and **7** are very similar. The Ag_6 units are both observed the two polymers. However, the Ag_6 units in **7** are infinite but not in **6** because the average coordination number for **7** is less than the one for **6**.

3.5 Thermogravimetric Analyses.

The thermal behaviors of **1-7** were studied by TGA (Fig. S3, ESI.†). The experiments were performed on the samples consisting of numerous single crystals under N_2 atmosphere with a heating rate of 10 °C min^{-1} . The TGA curves of compounds **1** and **2** display similar character. The decompositions of them start at about 230 and 270 °C, accompanying the release of the 2,5-dmpyz and carboxylate ligands. The TGA curves of **3-6** display similar character. The decompositions of them start at about 120-200 °C, accompanying the release of the 2,3-dmpyz and carboxylate ligands. For **7**, the CPs start to decompose at about 40 °C accompanying loss of lattice water molecules (Calcd. and found: 6.6% and 5.7%), then it does not decompose until the temperature reaches 242 °C, then the coordinated network begins to decompose, accompanying the release of the 2,3-dmpyz and tma ligands.

3.6 Photoluminescence properties

The Ag(I) CPs with aromatic ligands have received much attention for the development of chemical sensors, white light-emitting diodes (LEDs), and electroluminescent materials (OLEDs) for displays[52–58]. Thus, the photoluminescence properties of **1-7** as well as free ligand were investigated in the solid state at room temperature as shown in Fig. 5 and Fig. S4, ESI.†. The free ligands 2,5-dmpyz and 2,3-dmpyz display photoluminescence with emission maxima at 473 nm and 354 nm (λ_{ex} = 300 nm). It can be presumed that this peak originates from the $\pi^* \rightarrow n$ or $\pi \rightarrow \pi^*$ transitions[59]. Intense emissions are observed at 407 nm for **1**, 415 nm for **2**, 330 nm for **3**, 332 nm for **4**, 351 nm for **5**, 339 nm for **6** and 336 nm for **7** (λ_{ex} = 300 nm), respectively. The maximum emission wavelengths of compounds **1** and **2** undergo a blue shift. The emission bands of compounds **1** and **2** are mainly attributed to an intraligand emission state as reported for d^{10} metal compounds with N-donor ligands.[60] The intense emission bands for **3-7** are similar to that of the corresponding 2,3-dmpyz ligand probably due to the intraligand $\pi \rightarrow \pi^*$ transitions.[61] On the other hand,the Ag-Ag interactions have an important influence on the energy gap between the ground and excited states and have been reported as an important factor contributing to the photoluminescent properties of coinage d^{10} metal coordination compounds. So the different emissive behaviors may be arise from the synergistic effects of different interactions (such as hydrogen bonds and Ag-Ag interactions), which can result in the different HOMO-LUMO gap.[62–64]

4 Conclusion

Using 2,5-dmpyz and 2,3-dmpyz as ligands, seven new coordination compounds with different structures and dimensionalities from 2D networks to 3D frameworks were synthesized and structurally characterized. Interestingly, these seven CPs provide a way of understanding the versatile structures of silver units. The present work shows that the nitrogen-containing ligands and the carboxylate ligand play pivotal roles in the formation and determination of the silver units in the Ag containing polymers. The various structures of the silver units in the coordination polymers may be attributed to the different average coordination numbers and the complexity of coordination geometry around Ag(I). In our work, the silver ions with less coordination number and simpler coordination geometry tend to form more complex multinuclear Ag units in the coordination polymers.

Acknowledgments

This work was financially supported by the National Natural Science Foundation of China (No. 21071118).

References

1 W. Su, M. Hong, J. Weng, R. Cao and S. Lu, *Angewandte Chemie*, 2000, **112**, 3033–3036.
2 D. Sun, C.-F. Yang, H.-R. Xu, H.-X. Zhao, Z.-H. Wei, N. Zhang, L.-J. Yu, R.-B. Huang and L.-S. Zheng, *Chem. Commun.*, 2010, **46**, 8168–8170.
3 C. Seward, J. Chan, D. Song and S. Wang, *Inorg. Chem.*, 2003, **42**, 1112–1120.
4 S. Y. Ho, E. C.-C. Cheng, E. R. Tiekink and V. W.-W. Yam, *Inorg. Chem.*, 2006, **45**, 8165–8174.
5 L. Zhang, Z.-J. Li, Q.-P. Lin, Y.-Y. Qin, J. Zhang, P.-X. Yin, J.-K. Cheng and Y.-G. Yao, *Inorg. Chem.*, 2009, **48**, 6517–6525.
6 P. C. Zachariadis, S. K. Hadjikakou, N. Hadjiliadis, S. Skoulika, A. Michaelides, J. Balzarini and E. De Clercq, *Eur. J. Inorg. Chem.*, 2004, **2004**, 1420–1426.
7 K. Akhbari and A. Morsali, *Cryst. Growth Des.*, 2007, **7**, 2024–2030.
8 T. V. Slenters, J. L. Sagu, P. S. Brunetto, S. Zuber, A. Fleury, L. Mirolo, A. Y. Robin, M. Meuwly, O. Gordon and R. Landmann, *Materials*, 2010, **3**, 3407–3429.
9 G. K. Kole, C. K. Chin, G. K. Tan and J. J. Vittal, *Polyhedron*, 2013, **52**, 1440–1448.
10 S. Muthu, J. H. Yip and J. J. Vittal, *J. Chem. Soc., Dalton Trans.*, 2002, 4561–4568.
11 Q. Chu, D. C. Swenson and L. R. MacGillivray, *Angewandte Chemie*, 2005, **117**, 3635–3638.
12 R. Santra and K. Biradha, *Cryst. Growth Des.*, 2010, **10**, 3315–3320.
13 O.-S. Jung, Y. J. Kim, Y.-A. Lee, S. W. Kang and S. N. Choi, *Cryst. Growth Des.*, 2004, **4**, 23–24.

14 P.-p. Zhang, J. Peng, H.-j. Pang, J.-q. Sha, M. Zhu, D.-d. Wang, M.-g. Liu and Z.-m. Su, *Cryst. Growth Des.*, 2011, **11**, 2736–2742.

15 P.-S. Cheng, S. Marivel, S.-Q. Zang, G.-G. Gao and T. C. Mak, *Cryst. Growth Des.*, 2012, **12**, 4519–4529.

16 B. Li, S.-Q. Zang, H.-Y. Li, Y.-J. Wu and T. C. Mak, *J. Organomet. Chem.*, 2012, **708**, 112–117.

17 B. Li, R.-W. Huang, H.-C. Yao, S.-Q. Zang and T. C. Mak, *CrystEngComm*, 2014, **16**, 723–729.

18 B. Li, W.-K. Wang, S.-Q. Zang and T. C. Mak, *J. Organomet. Chem.*, 2013, **745**, 173–176.

19 R.-W. Huang, Y. Zhu, S.-Q. Zang and M.-L. Zhang, *Inorg. Chem. Commun.*, 2013.

20 D. Sun, G.-G. Luo, N. Zhang, Q.-J. Xu, C.-F. Yang, Z.-H. Wei, Y.-C. Jin, L.-R. Lin, R.-B. Huang and L.-S. Zheng, *Inorg. Chem. Commun.*, 2010, **13**, 290–293.

21 V. T. Yilmaz, E. Senel, E. Guney and C. Kazak, *Inorg. Chem. Commun.*, 2008, **11**, 1330–1333.

22 E. Soyer, F. Yilmaz, V. T. Yilmaz, O. Buyukgungor and W. T. Harrison, *J. Inorg. Organomet. Polym Mater.*, 2010, **20**, 320–325.

23 L. Brammer, M. D. Burgard, M. D. Eddleston, C. S. Rodger, N. P. Rath and H. Adams, *CrystEngComm*, 2002, **4**, 239–248.

24 M. A. M. Abu-Youssef, V. Langer and L. Ohrstrom, *Dalton Trans.*, 2006, 2542–2550.

25 H.-Y. Liu, H. Wu, J.-F. Ma, J. Yang and Y.-Y. Liu, *Dalton Trans.*, 2009, 7957–7968.

26 H.-Y. Liu, H. Wu, J.-F. Ma, S.-Y. Song, J. Yang, Y.-Y. Liu and Z.-M. Su, *Inorg. Chem.*, 2007, **46**, 7299–7311.

27 M. Rigaku, *Rigaku/MSC, The Woodlands, TX*, 2004.

28 T. Higashi, *Matsubara, Akishima, Japan*, 1995, 9–12.

29 S. Bruker, *Bruker AXS Inc., Madison, Wisconsin, USA*, 1998.

30 G. Sheldrick, *Gottingen University, Germany*, 1997.

31 G. Sheldrick, *Gottingen University, Germany*, 1997.

32 O. V. Dolomanov, L. J. Bourhis, R. J. Gildea, J. A. Howard and H. Puschmann, *J. Appl. Crystallogr.*, 2009, **42**, 339–341.

33 A. Spek, *Utrecht University, Utrecht, The Netherlands*, 1998.

34 K. Nakamoto, *Infrared and Raman spectra of inorganic and coordination compounds*, Wiley Online Library, 1978.

35 L. Yang, D. R. Powell and R. P. Houser, *Dalton Trans.*, 2007, **9**, 955–964.

36 A. Bondi, *The Journal of Physical Chemistry*, 1964, **68**, 441–451.

37 A. Addison, T. Rao and J. Reedijk, *Dalton Trans.*, 1984, 1349–1356.

38 C. Streb, C. Ritchie, D. Long, P. Kgerler and L. Cronin, *Angewandte Chemie*, 2007, **119**, 7723–7726.

39 J. Fielden, D.-l. Long, A. M. Slawin, P. Kgerler and L. Cronin, *Inorg. Chem.*, 2007, **46**, 9090–9097.

40 I. J. Lin and C. S. Vasam, *Coord. Chem. Rev.*, 2007, **251**, 642–670.

41 Y.-P. Xie and T. C. Mak, *J. Am. Chem. Soc.*, 2011, **133**, 3760–3763.

42 B. Li, S.-Q. Zang, C. Ji, C.-X. Du, H.-W. Hou and T. C. Mak, *Dalton Trans.*, 2011, **40**, 788–792.

43 Z.-H. Wang, S.-F. Chen, D.-F. Wang, H.-J. Hao, H.-X. Mei, R.-B. Huang and L.-S. Zheng, *J. Mol. Struct.*, 2013, **1050**, 97–102.

44 A. N. Khlobystov, A. J. Blake, N. R. Champness, D. A. Lemenovskii, A. G. Majouga, N. V. Zyk and M. Schrder, *Coord. Chem. Rev.*, 2001, **222**, 155–192.

45 B. R. Bhogala, P. K. Thallapally and A. Nangia, *Cryst. Growth Des.*, 2004, **4**, 215–218.

46 P. J. Steel and C. M. Fitchett, *Coord. Chem. Rev.*, 2008, **252**, 990–1006.

47 C.-L. Chen, B.-S. Kang and C.-Y. Su, *Aust. J. Chem.*, 2006, **59**, 3–18.

48 M. Pascu, F. Tuna, E. Kolodziejczyk, G. I. Pascu, G. Clarkson and M. J. Hannon, *Dalton Trans.*, 2004, 1546–1555.

49 Y.-L. Wang, Q.-Y. Liu and L. Xu, *CrystEngComm*, 2008, **10**, 1667–1673.

50 C.-J. Wu, C.-Y. Lin, P.-C. Cheng, C.-W. Yeh, J.-D. Chen and J.-C. Wang, *Polyhedron*, 2011, **30**, 2260–2267.

51 Y. Zhou, W. Chen and D. Wang, *Dalton Trans.*, 2008, 1444–1453.

52 Y.-D. Chen, Y.-H. Qin, L.-Y. Zhang, L.-X. Shi and Z.-N. Chen, *Inorg. Chem.*, 2004, **43**, 1197–1205.

53 G. De Santis, L. Fabbrizzi, M. Licchelli, A. Poggi and A. Taglietti, *Angew. Chem., Int. Ed. Engl.*, 1996, **35**, 202–204.

54 J.-L. Liu and B. Yan, *Dalton Trans.*, 2011, **40**, 1961–1968.

55 G.-E. Wang, M.-S. Wang, M.-J. Zhang, L.-Z. Cai, B.-W. Liu, C.-J. Zhang, G.-C. Guo and J.-S. Huang, *Inorg. Chem. Commun.*, 2012.

56 G.-N. Liu, X.-M. Jiang, M.-F. Wu, G.-E. Wang, G.-C. Guo and J.-S. Huang, *Inorg. Chem.*, 2011, **50**, 5740–5746.

57 M.-S. Wang, S.-P. Guo, Y. Li, L.-Z. Cai, J.-P. Zou, G. Xu, W.-W. Zhou, F.-K. Zheng and G.-C. Guo, *J. Am. Chem. Soc.*, 2009, **131**, 13572–13573.

58 X. Liu, K.-L. Huang, G.-M. Liang, M.-S. Wang and G.-C. Guo, *CrystEngComm*, 2009, **11**, 1615–1620.

59 W. Chen, J.-Y. Wang, C. Chen, Q. Yue, H.-M. Yuan, J.-S. Chen and S.-N. Wang, *Inorg. Chem.*, 2003, **42**, 944–946.

60 L. Yi, L.-N. Zhu, B. Ding, P. Cheng, D.-Z. Liao, S.-P. Yan and Z.-H. Jiang, *Inorg. Chem. Commun.*, 2003, **6**, 1209–1212.

61 X.-Q. Fang, Z.-P. Deng, L.-H. Huo, W. Wan, Z.-B. Zhu, H. Zhao and S. Gao, *Inorg. Chem.*, 2011, **50**, 12562–12574.

62 V. Wing-Wah Yam and K. Kam-Wing Lo, *Chem. Soc. Rev.*, 1999, **28**, 323–334.

63 V. T. Yilmaz, S. Hamamci, S. Gumus and O. Bykgngr, *J. Mol. Struct.*, 2006, **794**, 142 – 147.

64 S.-L. Zheng, J.-P. Zhang, W.-T. Wong and X.-M. Chen, *J. Am. Chem. Soc.*, 2003, **125**, 6882–6883.

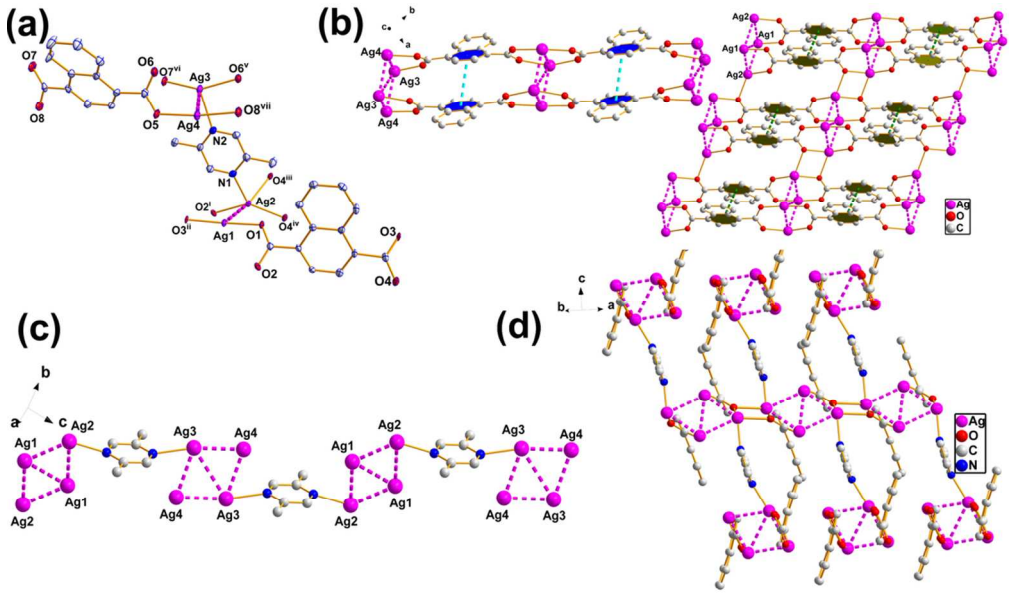

Fig. 1 (a) The coordination environment of Ag (I) ions in **1** with the thermal ellipsoids at 50% probability level. Hydrogen atoms are omitted for clarity. (b) View of the 1D chain and 2D sheet of complex **1**. (c) Schematic representation of the Ag4 baskets. (d) Schematic representation of the 3D framework including Ag•••Ag interactions (pink dashed lines). (Symmetry codes: (i) 1−x, 2−y, 1−z; (ii) −1+x, −1+y, z; (iii) x, −1+y, z; (iv) 2−x 3−y, 1−z; (v) 1−x, 1−y, −z; (vi) −x, −y, −z; (vii) 1+x, 1+y, z.)
101x60mm (300 x 300 DPI)

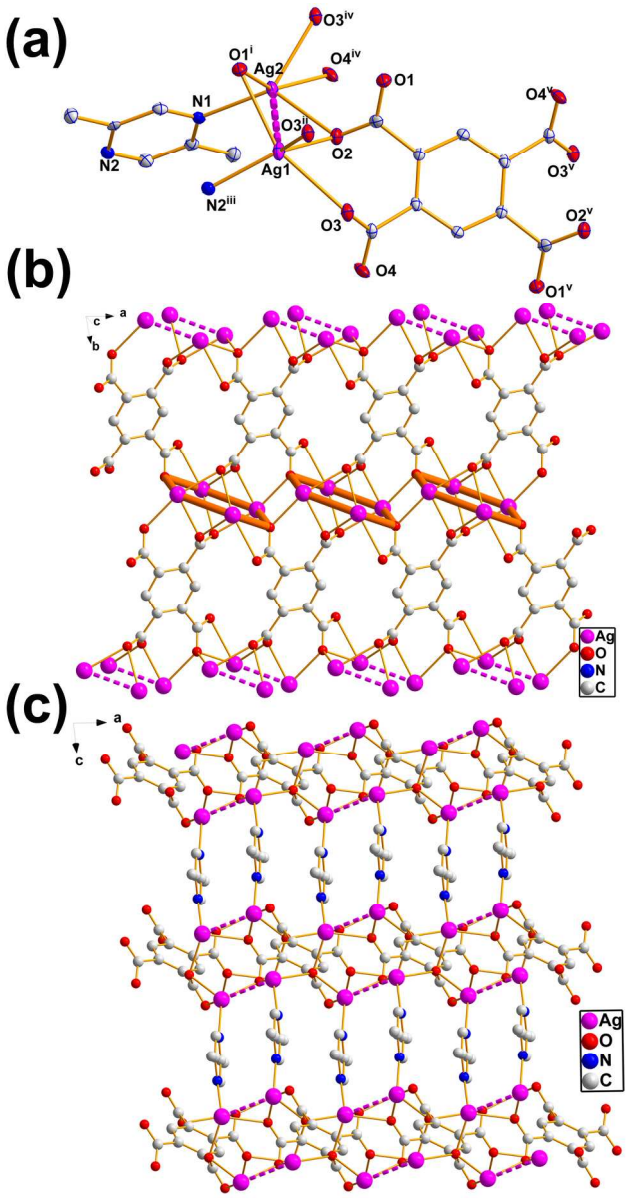

Fig. 2 (a) The coordination environment of Ag (I) ions in **2** with the thermal ellipsoids at 50% probability level. Hydrogen atoms are omitted for clarity. (b) The 2D net in **2** including $[Ag_4O_2]$ units. (c) The 3D supramolecular structure extended from 2D nets through dmpyz ligand. (Symmetry codes: (i) −x, 2−y, −z; (ii) 1−x, 2−y, −z; (iii) −x, 2−y, 1−z; (iv) −1+x, y, z; (v) x+1, y, z.)
143x246mm (300 x 300 DPI)

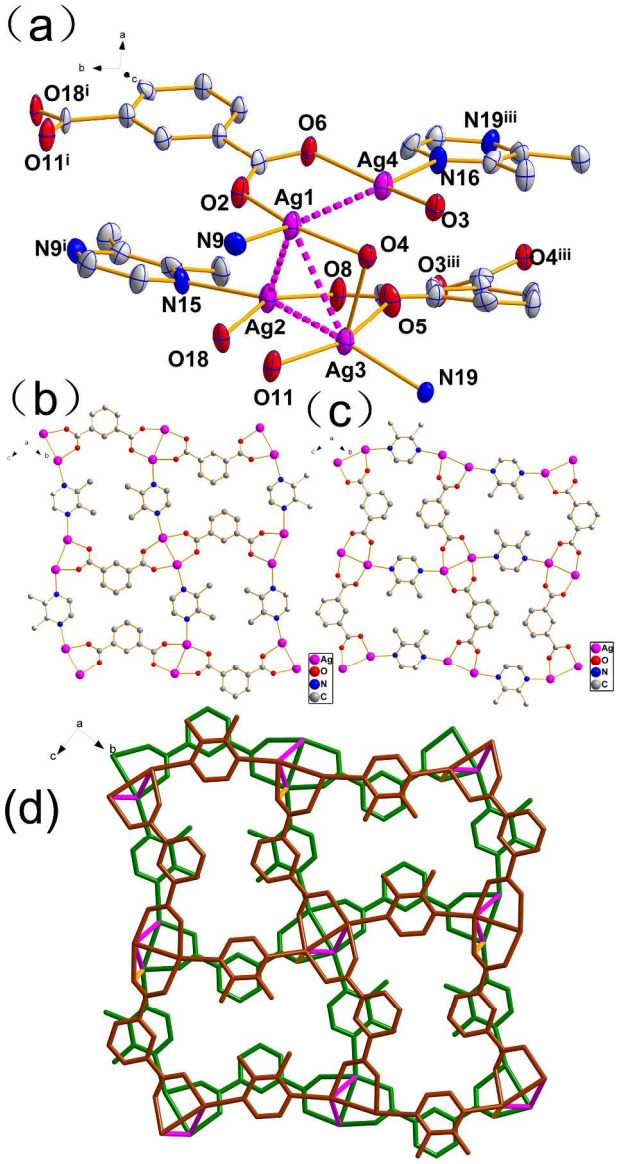

Fig. 3 (a) The coordination environment of Ag (I) ions in **3** with the thermal ellipsoids at 50% probability level. Hydrogen atoms are omitted for clarity. (b) The 2D net cooperated by Ag1 and Ag4. (c) The 2D net cooperated by Ag2 and Ag3. (d) The double layer combined by the two kinds of networks. (Symmetry codes: (i) –x, 2−y, −1/2+z; (iii) –x, 1−y, −1/2+z.)
162x318mm (300 x 300 DPI)

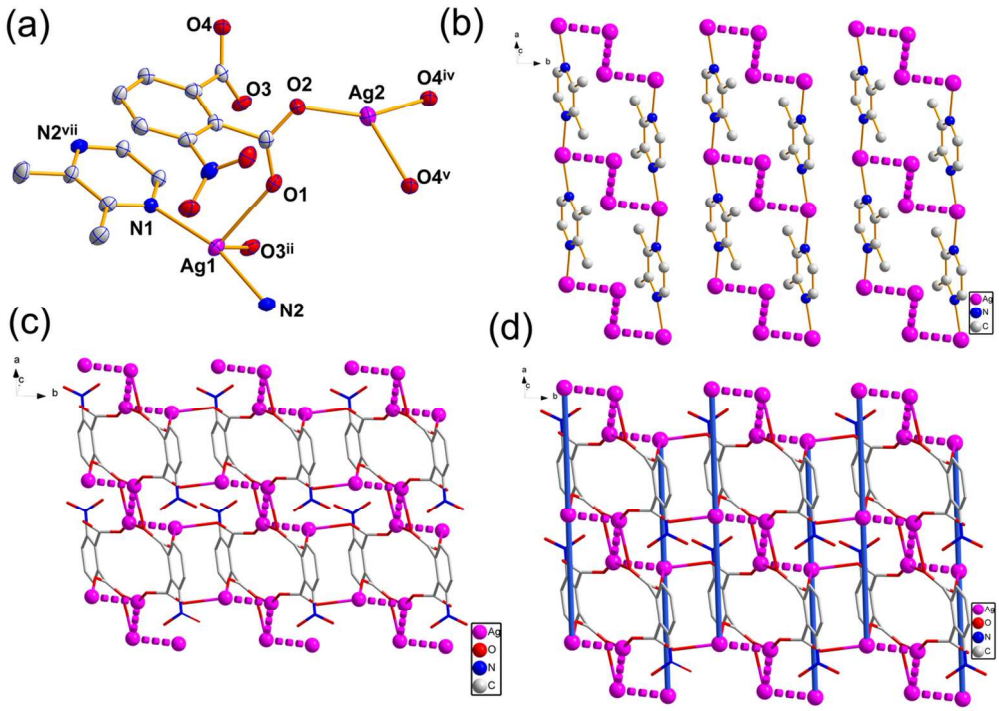

Fig. 4 (a) The coordination environment of Ag (I) ions in **4** with the thermal ellipsoids at 50% probability level. Hydrogen atoms are omitted for clarity. (b) The chains along the a axis formed by 2,3-dmpyz and Ag_4 units. (c) The 2D network consolidated by npa ligands. (d) Ball-and-stick view of resulting 2D sheet. (Symmetry codes: (ii) −x, 1−y, −z; (iv) −x, 2−y, −z (v) 1+x, y, z; (vii) −1+x, y, z.)
120x84mm (300 x 300 DPI)

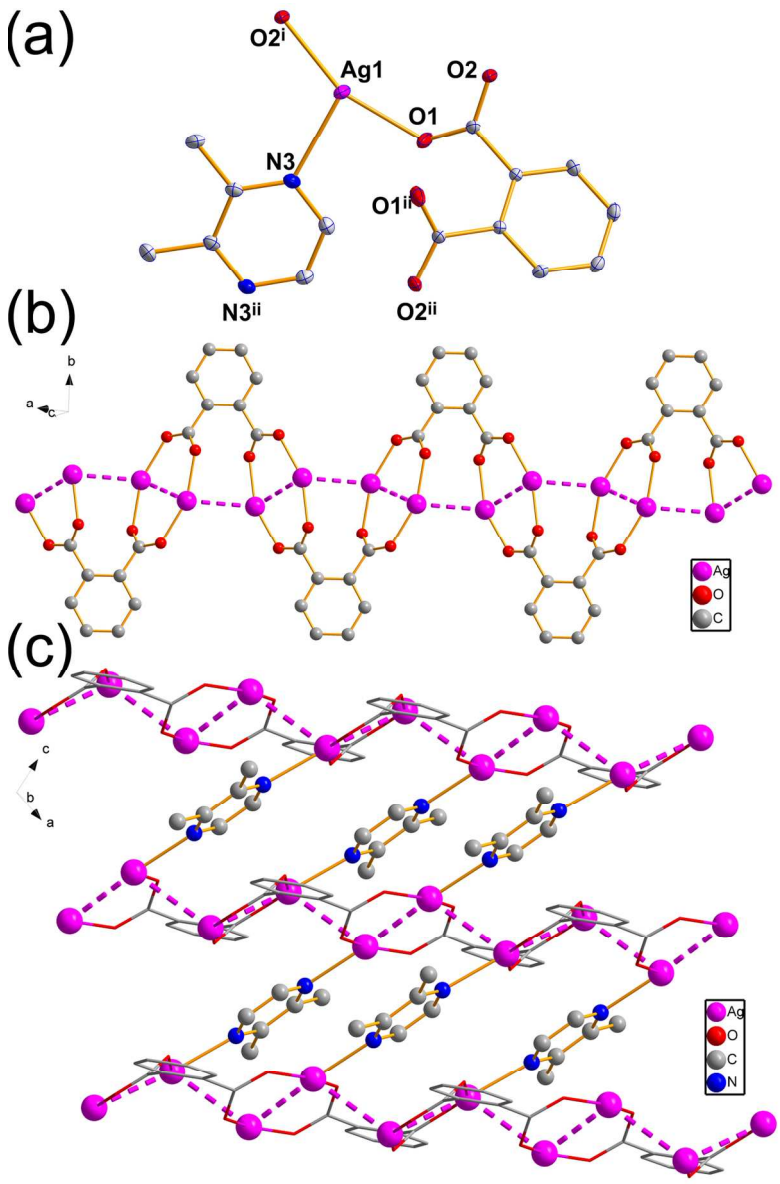

Fig. 5 (a) The coordination environment of Ag (I) ions in **5** with the thermal ellipsoids at 50% probability level. Hydrogen atoms are omitted for clarity. (b) Presentation of 1D infinite Ag chain. (c) Ball-and-stick view of 2D sheet. (Symmetry codes: (i) −x+2, y, −z+1/2; (ii) −x+3/2, −y+1/2, −z.)
129x200mm (300 x 300 DPI)

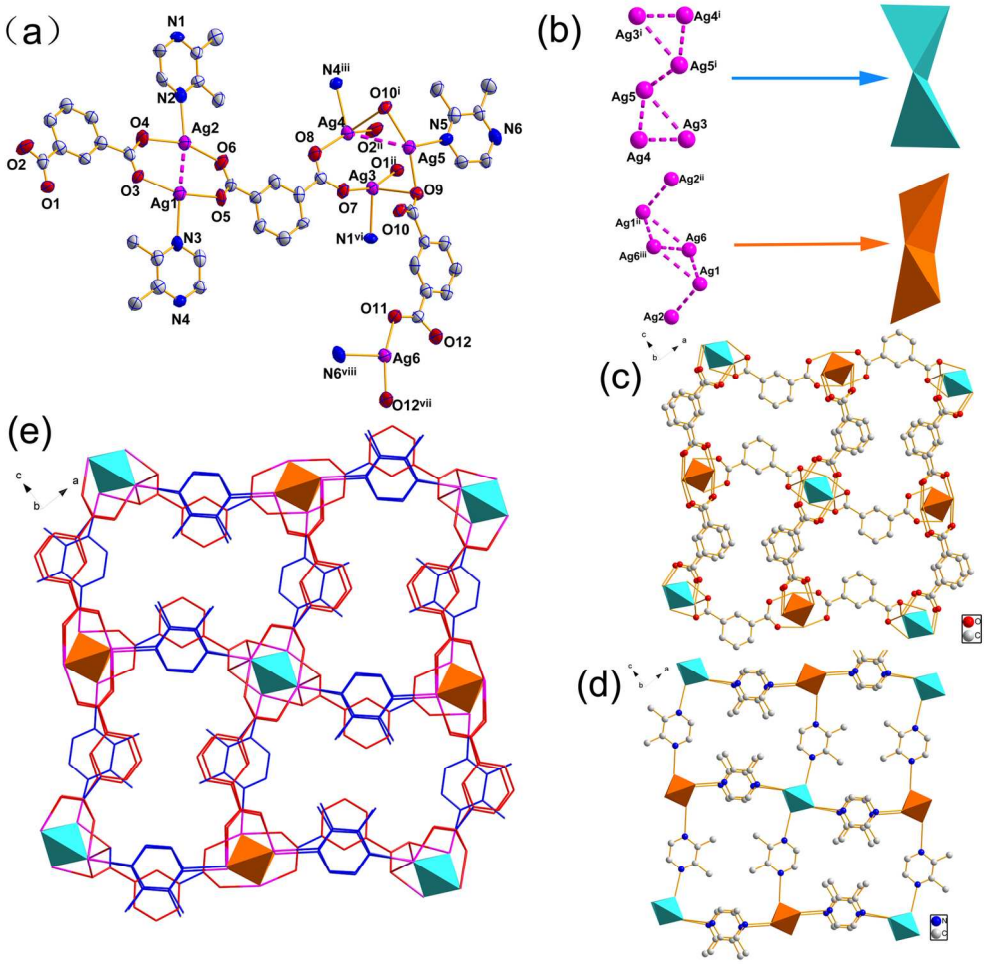

Fig. 6 (a) The coordination environment of Ag (I) ions in **6** with the thermal ellipsoids at 50% probability level. Hydrogen atoms are omitted for clarity. (b) View of the two types of Ag units. (c) The 2D network consolidated by mpa ligands. (d) The 2D network consolidated by 2,3-dmpyz ligands. (e) View of the resulting 2D structure (red line: mpa ligand; blue line: 2,3-dmpyz ligand). (Symmetry codes: (i) −x−1, −y, −z−1; (ii) x−1, y, z−1; (iii) x−1, y, z; (vi) x, y, z−1; (vii) −x, −y, −z−2; (viii) x+1, y, z.)
166x161mm (300 x 300 DPI)

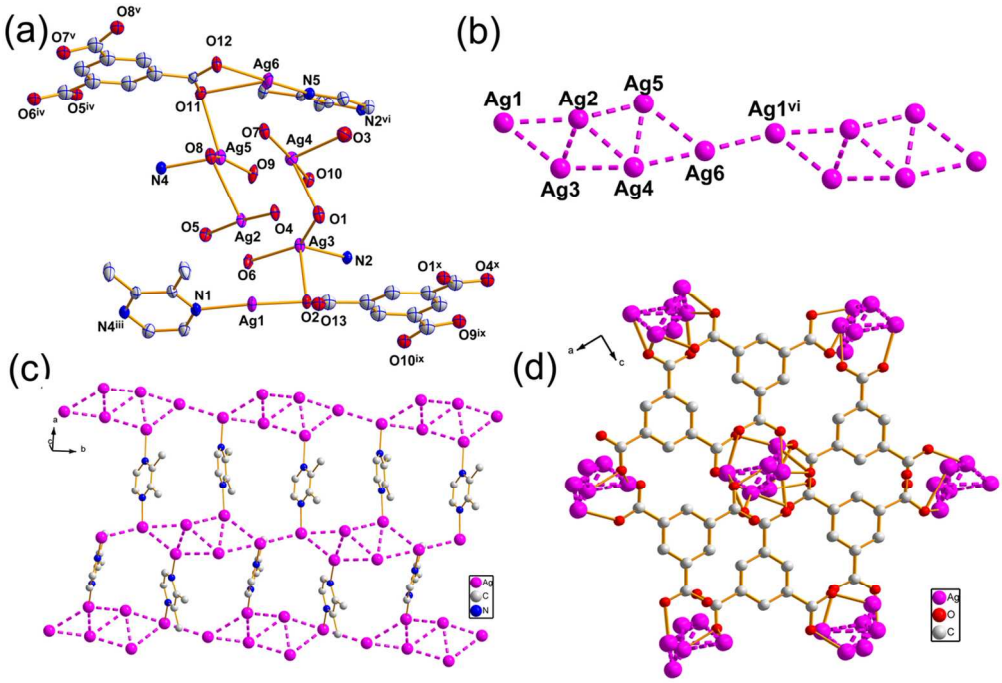

Fig. 7 (a) The coordination environment of Ag (I) ions in **7** with the thermal ellipsoids at 50% probability level. Hydrogen atoms are omitted for clarity. (b) View of the infinite Ag strap. (c) The 2D network consolidated by 2,3-dmpyz. (d) 3D supramolecular architecture constructed by tma ligands. (Symmetry codes: (iii) –x, –1/2+y, 1/2–z; (iv) –x, 1/2+y, 1/2–z; (v) –x, 2–y, 1–z; (vi) 1–x, 1/2+y, 1/2–z; (ix) 1–x, –1/2+y, 1/2–z; (x) 1–x, 1–y, 1–z.)
116x78mm (300 x 300 DPI)

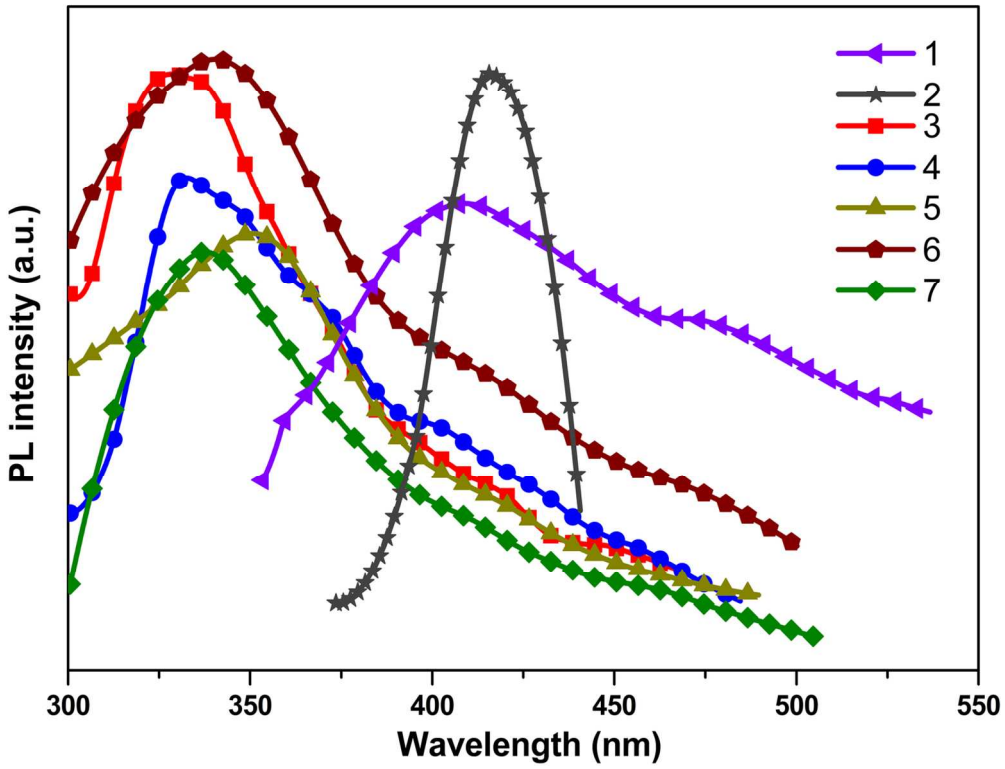

Fig. 8 Photoluminescence properties of CPs **1–7**.
65x50mm (600 x 600 DPI)

Table 1 Pertinent crystallographic data collections and refinement parameters[a]

Compound	**1**	**2**	**3**	**4**	**5**	**6**	**7**
Empirical formula	$Ag_4C_{30}H_{20}N_2O_8$	$Ag_2C_{11}H_9N_2O_4$	$Ag_4C_{28}H_{24}N_4O_8$	$Ag_2C_{14}H_{11}N_3O_6$	$AgC_7H_6NO_2$	$Ag_6C_{42}H_{36}N_6O_{12}$	$Ag_6C_{30}H_{32}N_4O_{17}$
Formula weight	967.96	448.94	975.99	533.00	244.00	1463.99	1367.82
Crystal system	triclinic	triclinic	orthorhombic	monoclinic	monoclinic	monoclinic	monoclinic
Space group	*P*-1	*P*-1	$Pca2_1$	$P2_1/c$	*C*2/c	$P2_1/c$	$P2_1/c$
a/Å	8.059(2)	6.483(2)	13.687(2)	7.2517(14)	9.3459(19)	14.757(3)	16.306(2)
b/Å	10.243(4)	9.222(4)	14.880(3)	7.7768(15)	21.924(4)	20.578(4)	11.578(4)
c/Å	17.378(3)	10.555(3)	13.809(4)	25.608(4)	7.0573(14)	13.995(2)	19.417(3)
α/°	98.88	64.498	90.00	90.00	90.00	90.00	90.00
β/°	96.736(4)	81.417(4)	90.00	90.522(4)	106.11(3)	90.040(4)	90.207(4)
γ/°	105.14	80.977	90.00	90.00	90.00	90.00	90.00
V/Å^3	1349.4(7)	560.1(3)	2812.4(11)	1444.1(5)	1389.2(5)	4249.9(13)	3665.5(16)
Z, D_{calcd} (Mg/m^3)	2, 2.382	2, 2.6616	4, 2.305	4, 2.4513	8, 2.333	4, 2.288	4, 2.479
m/mm^{-1}	2.919	3.507	2.804	2.754	2.838	2.783	3.225
F(000)	932	430	1888	1025.2	944	2832	2632
Reflections collected	13421	4516	26285	13821	6641	39010	33673
Independent reflections	6141	2034	6424	3299	1590	9705	8372
Data/restraints/parameters	6141/0/399	2034/0/174	6424/1/403	3299/0/227	1590/0/100	9705/0/602	8372/0/522
Goodness-of-fit on F^2	1.082	1.102	1.000	1.022	1.115	1.01	1.182
R_{int}	0.0795	0.035	0.1199	0.0691	0.0497	0.1137	0.0422
Final *R* indexes[a] [$I>=2\sigma(I)$]	R_1 = 0.0408, wR_2 = 0.1079	R_1 = 0.0270, wR_2 = 0.0651	R_1 = 0.0600, wR_2 = 0.1318	R_1 = 0.0395, wR_2 = 0.0823	R_1 = 0.0294, wR_2 = 0.0743	R_1 = 0.0818, wR_2 = 0.1963	R_1 = 0.0298, wR_2 = 0.0748
Final *R* indexes [all data]	R_1 = 0.0546, wR_2 = 0.1133	R_1 = 0.0305, wR_2 = 0.0689	R_1 = 0.0824, wR_2 = 0.1496	R_1 = 0.0580, wR_2 = 0.0977	R_1 = 0.0324, wR_2 = 0.0775	R_1 =0.1410, wR_2 = 0.2676	R_1 = 0.0361, wR_2 = 0.0776
Largest diff. peak/hole / e·Å^{-3}	2.04/-2.18	1.13/-0.84	1.82/-1.56	1.13/-1.51	0.83/-2.20	2.25/-2.43	1.15/-1.67

[a] $R_1 = \Sigma| |F_o|-|F_c| | / \Sigma|F_o|$, $wR_2 = [\Sigma w(F_o^2-F_c^2)^2] / \Sigma w(F_o^2)^2]^{1/2}$

Table 2 Selected bond lengths and angles of Ag···Ag interaction for **1–7**

Compound **1**							
Ag1—Ag1^{i}	3.0048(9)	Ag3—Ag3^{v}	3.3696(10)	Ag1—Ag2^{i}	2.8533(7)	Ag3—Ag4^{v}	2.8383(8)
Ag1—Ag2	3.0631(9)	Ag3—Ag4	2.9671(10)				
Ag1^{i}—Ag1—Ag2	56.089(16)	Ag2^{i}—Ag1—Ag1^{i}	62.99(2)	Ag2^{i}—Ag1—Ag2	119.08(2)	Ag1^{i}—Ag2—Ag1	60.92(2)
Ag4—Ag3—Ag3^{v}	52.756(16)	Ag4^{v}—Ag3—Ag3^{v}	56.32(2)	Ag4^{v}—Ag3—Ag4	109.08(2)	Ag3^{v}—Ag4—Ag3	70.92(2)
Symmetry codes: (i) 1−x, 2−y, 1−z; (v) 1−x, 1−y, −z.							
Compound **2**							
Ag1—Ag2	3.1697(9)						
Ag2—Ag1—Ag2^{i}	90.618(15)	Ag1—Ag2—Ag1^{i}	89.382(15)				
Symmetry codes: (i) −x, 2−y, −z.							
Compound **3**							
Ag1—Ag2	3.1103(12)	Ag1—Ag3	3.1532(12)	Ag1—Ag4	2.9507(12)		
Ag2—Ag1—Ag3	57.51(3)	Ag4—Ag1—Ag2	82.69(3)	Ag4—Ag1—Ag3	85.11(3)	Ag2—Ag3—Ag1	60.53(3)
Ag3—Ag2—Ag1	61.96(3)						
Compound **4**							
Ag1^{i}—Ag2	3.0051(7)	Ag2^{iii}—Ag2	3.1628(10)				
Ag2^{iii}—Ag2—Ag1^{vi}	108.49(2)						
Symmetry codes: (i) x, −1+y, z; (iii) 1−x, 2−y, −z; (iv) −x, 2−y, −z.							
Compound **5**							
Ag1—Ag1^{i}	3.2448(9)	Ag1—Ag1^{ii}	2.9366(9)				
Ag1^{ii}—Ag1—Ag1^{i}	112.00(3)						
Symmetry codes: (i) −x+2, y, −z+1/2; (ii) −x+3/2, −y+1/2, −z.							
Compound **6**							
Ag1—Ag6^{iv}	3.0539(14)	Ag1—Ag6^{v}	3.3885(14)	Ag1—Ag2	2.9512(16)	Ag3—Ag5	3.1485(14)
Ag4—Ag3	2.9510(14)	Ag4—Ag5	3.2731(13)	Ag6—Ag6^{vii}	3.0053(19)	Ag5—Ag5^{i}	2.9297(19)
Ag6^{iv}—Ag1—Ag6^{v}	55.32(3)	Ag2—Ag1—Ag6^{v}	88.69(4)	Ag4—Ag3—Ag5	64.81(3)	Ag3—Ag4—Ag5	60.51(3)
Ag5^{i}—Ag5—Ag4	82.51(4)	Ag5^{i}—Ag5—Ag3	81.58(4)	Ag3—Ag5—Ag4	54.67(3)	Ag1^{vi}—Ag6—Ag1^{v}	124.68(3)
Ag6^{vii}—Ag6—Ag1^{v}	56.68(3)	Ag6^{vii}—Ag6—Ag1^{vi}	68.00(4)				
Symmetry codes: (i) −x−1, −y, −z−1; (iv) x, y, z+1; (v) −x, −y, −z−1; (vi) x, y, z−1; (vii) −x, −y, −z−2.							
Compound **7**							
Ag1—Ag6^{ii}	3.3326(12)	Ag2—Ag5	3.2128(11)	Ag2—Ag1	3.1823(12)	Ag2—Ag4	3.1638(8)
Ag2—Ag3	2.9179(5)	Ag5—Ag4	2.8531(5)	Ag3—Ag4	3.3519(10)	Ag4—Ag6	3.0846(11)
Ag2—Ag1—Ag6^{ii}	148.299(19)	Ag3—Ag2—Ag5	93.609(12)	Ag3—Ag2—Ag4	66.748(16)	Ag3—Ag2—Ag1	68.405(10)
Ag4—Ag2—Ag5	53.151(18)	Ag4—Ag2—Ag1	132.797(18)	Ag1—Ag2—Ag5	144.154(18)	Ag2—Ag3—Ag4	60.139(10)
Ag2—Ag4—Ag3	53.113(17)	Ag5—Ag4—Ag3	91.922(13)	Ag6—Ag4—Ag2	124.81(2)	Ag6—Ag4—Ag3	157.180(15)
Ag5—Ag4—Ag2	64.304(16)	Ag5—Ag4—Ag6	70.304(12)	Ag4—Ag5—Ag2	62.545(10)	Ag4—Ag6—Ag1^{i}	154.001(17)
Symmetry codes: (i) x, y+1, z; (ii) x, y−1, z.							